

# Calculation Methods for Radio Pulses from High Energy Showers

J. Alvarez-Muñiz

*Department of Physics, University of Wisconsin, Madison, WI 53706, USA*

R.A. Vázquez and E. Zas

*Departamento de Física de Partículas, Universidade de Santiago*

*E-15706 Santiago de Compostela, Spain*

## Abstract

We present an approximation for the numerical calculation of Čerenkov radio pulses in the Fraunhofer limit from very high energy showers in dense media. We compare it to full Montecarlo simulations in ice studying its range of applicability and show how it can be extended with a simple algorithm. The approximation reproduces well the angular distribution of the pulse around the Čerenkov direction. An improved parameterization for the frequency spectrum in the Čerenkov direction is given for phenomenological applications. We extend the method to study the pulses produced by showers at distances at which the Fraunhofer limit does not apply, and give the ranges of distances and frequencies in which Fraunhofer approximation is good enough for interpreting future experimental data. Our results are relevant for the detection of very high energy neutrinos with this technique.

**PACS number(s):** 96.40.Pq; 96.40.Tv; 95.85.Bh; 13.15.+g

**Keywords:** Čerenkov radiation, LPM effect, Electromagnetic and hadronic showers, Neutrino detection.

## I. INTRODUCTION

The confirmed detection of cosmic rays above the Greisen-Zatsepin-Kuz'min cutoff gives confidence in the existence of neutrinos of energies reaching the EeV scale and above. Such neutrinos are expected both in models in which the protons are accelerated to the highest energies [1], such as in Active Galactic Nuclei [2] or Gamma Ray Bursts [3] and in “top bottom” scenarios [4,5] in which cosmic rays are basically produced through quark fragmentation in events such as the decay of long lived heavy relic particles [6] or the annihilation of topological defects [7]. If the highest energy component of the cosmic rays are protons, as suggested by increasing experimental evidence [8–10], they are expected to produce neutrinos in their interactions with the cosmic microwave background [11]. Neutrino detection would provide extremely valuable information on fundamental questions, both in astrophysics, such as the origin of the highest energy cosmic rays and in particle physics.

Detecting high energy neutrinos may be a reality in the immediate future as many efforts are being made to develop large scale Čerenkov detectors under water or ice [12], designed to challenge the low neutrino cross section exploiting the long range of the high energy muons produced in charged current muon neutrino interactions. For EeV neutrinos these detectors are also capable of detecting light from high energy showers produced by neutrinos of any flavor in both neutral and charged current interactions, but the effective acceptance of the detector is reduced because the shower must be produced very close or within the instrumented volume.

It has been known for long that the development of showers in dense media produces an excess charge which generates a coherent Čerenkov pulse in the radiowave frequency when it propagates through the medium [13]. The detection of these pulses provides a possible alternative to neutrino detection particularly appropriate for very high energies [14–16] because the signal scales with the square of the primary energy [17,24]. The method is attractive because of the good transmission properties of large natural volumes of ice and sand and because much information about the charge distribution in the shower is

preserved in the frequency and angular distribution of the pulses. This last property can be used to extract information about shower energy and neutrino flavor [18]. The technique faces a number of technical difficulties however [19] and several attempts are currently being made to test the theoretical predictions [20] and to study the feasibility of the technique in Antarctic ice [21].

Theoretical calculations are also difficult because a complete interference calculation calls for simulations capable of following electrons and positrons to the Čerenkov threshold ( $\sim 100$  keV). For high energy showers this is unfortunately out of question because of the large number of particles involved and approximations have been specifically devised to study the radio emission of high energy showers in ice. The calculation of radio pulses from EeV showers has been possible in the *one dimensional* (1-D) *approximation* which consists on neglecting both the lateral distribution and the subluminal velocity of shower particles [18,22,23]. All the calculations of radio pulses have been made so far in the Fraunhofer limit. In this limit the dependence of the electric field on distance to shower is trivial and the characterization of the angular distribution of the radio pulse at a given frequency is effectively only dependent on one variable, namely the angle between the shower axis and the observation direction what simplifies the simulations [24]. Clearly Fresnel type interference will take place if the showers are close enough to the detectors, but the calculation of these effects becomes even more time consuming.

In this paper we firstly give a brief introduction to coherent radio emission in Section II (fuller details can be found in Refs. [24,25]) accounting for the approximations made. In Section III we make extensive tests and explore the validity of the 1-D approximation in the Fraunhofer limit by direct comparison with complete simulations, and we discuss the approximation pointing out the connections between the radio emission and shower fluctuations, what gives new and useful insight into the radioemission processes. In Section IV we use the 1-D approximation without taking the Fraunhofer limit to study the radiopulse as a function of the distance to observation point. In Section V we summarize and conclude, commenting on the implications of our results for neutrino detection.

## II. ČERENKOV RADIO PULSES

When a charged particle travels through a dielectric medium of refraction index  $n$  with speed  $\beta c$  greater than the phase velocity of light in that medium ( $c/n$ ), then Čerenkov radiation is emitted in a frequency band over which the  $\beta n > 1$  condition is satisfied without large absorbtion. The calculation of the Čerenkov electric field associated to the particle is a problem of classical electromagnetism that has been addressed elsewhere [26]. Solving the inhomogeneous Maxwell's equations in the transverse gauge, it is easy to obtain the Fourier components of the electric field produced by a current density  $\vec{J}(\vec{x}', t')$ :

$$\vec{E}(\vec{x}, \omega) = \frac{e\mu_r}{2\pi\epsilon_0 c^2} i\omega \int \int \int dt' d^3\vec{x}' \frac{e^{i\omega t' + ik|\vec{x} - \vec{x}'|}}{|\vec{x} - \vec{x}'|} \vec{J}_\perp(\vec{x}', t') \quad (1)$$

where  $\vec{J}_\perp(\vec{x}', t')$  is the component of the current transverse to the direction of observation  $\vec{x}$ . Also  $\nu$  ( $\omega$ ) is the frequency (angular frequency),  $k$  is the modulus of the wave vector  $\vec{k}$ ,  $\mu_r$  is the relative permeability of the medium and  $\epsilon_0$  and  $c$  is the permittivity and velocity of light in the vacuum.

A powerful approach to the simulation problem can be obtained neglecting the lateral distributions in shower particles and assuming all particles move at constant speed  $c$  in one dimension. We obtain a useful compact expression relating the charge distribution of the shower and its associated electric field. Crude as it may look, this approximation (1-D approximation in brief) will be shown to give very good results particularly around the Čerenkov angle and it has allowed the possibility of establishing the radioemission from EeV showers [22,23]. The method naturally relates different features of shower development to the spectrum and angular distribution of the radio emission in an interesting way, giving insight into the complexity of the calculated angular pulses. For simplicity we are going to take  $\vec{x}' = \vec{z}' = z'\hat{n}_{z'}$  where  $\hat{n}_{z'}$  is a unitary vector along the shower axis. The current associated to the shower development in this approximation is then given by:

$$\vec{J}_\perp(\vec{z}', t') = Q(z') \vec{e}_\perp \delta^3(\vec{z}' - \vec{c}t') \quad (2)$$

where  $Q(z')$  is the longitudinal development of the excess charge in the shower. The substitution of this current into Eq. 1 leads to:

$$\vec{E}(\vec{x}, \omega) = \frac{e\mu_r}{2\pi\epsilon_0 c^2} i\omega \sin\theta \hat{n}_\perp \int dz' Q(z') \frac{e^{i\frac{\omega}{c}z' + ik|\vec{x} - z'\hat{n}_z|}}{|\vec{x} - z'\hat{n}_z|} \quad (3)$$

where  $\theta$  is the angle between the shower axis and the direction of observation  $\vec{x}$  and  $\hat{n}_\perp$  is a unitary vector perpendicular to  $\vec{x}$ .

We can use this expression to obtain the Čerenkov electric field emitted by a particle shower propagating along a medium. Eq. 3 accounts for the correct phase factors and distances for showers that are close to the observer (Fresnel region). In the Fraunhofer limit the phase factor in Eq. 3 can be approximated by  $ik|\vec{x} - \vec{z}'| \simeq ikR - i\vec{k}\vec{z}'$ , where  $R = |\vec{x}|$  is the distance from the center of the shower to the observation point. It corresponds to the condition that observation distance  $R$  exceeds the Fresnel distance  $R_F = \pi n \nu (L_s \sin\theta/2)^2/c$ , where  $L_s$  is the typical length of the shower. In this limit it is straightforward to show that the electric field emitted by a shower in the 1-D approximation can be related to the Fourier transform of the longitudinal charge distribution:

$$\vec{E}(\omega, \vec{x}) = \frac{e\mu_r}{2\pi\epsilon_0 c^2} i\omega \sin\theta \frac{e^{ikR}}{R} \hat{n}_\perp \int dz' Q(z') e^{ipz'} \quad (4)$$

where we have introduced for convenience the parameter  $p(\theta, \omega) = (1 - n \cos\theta) \omega/c$  in Eq. 4 to stress the connection between the radio emission spectrum and the Fourier transform of the (excess) charge distribution. This allows a simple analogy to the classical diffraction pattern of an aperture function and helps understanding many of the complex features of the results obtained by simulation.

For the case of a single particle moving between two fixed points this expression (replacing  $c$  by an arbitrary particle velocity  $v$ ) reproduces the formula obtained in [24]:

$$\vec{E}(\omega, \vec{x}) = \frac{e\mu_r}{2\pi\epsilon_0 c^2} \frac{i\omega}{R} \frac{e^{ikR}}{R} \vec{v}_\perp \left[ \frac{e^{i(\omega - \vec{k} \cdot \vec{v})t_2} - e^{i(\omega - \vec{k} \cdot \vec{v})t_1}}{i(\omega - \vec{k} \cdot \vec{v})} \right] \quad (5)$$

where  $\vec{v}_\perp$  refers to the particle's velocity projected in a plane perpendicular to the observing direction and  $t_2$  ( $t_1$ ) is the time corresponding to the final (initial) point of the track. This is

the basic expression used for the numerical simulation of radio pulses from individual tracks (see appendix A).

### III. THE ONE-DIMENSIONAL APPROACH

We will firstly explore the validity of the 1-D approximation by direct comparison with simulation results in three dimensions. The program we use for the full simulation of electromagnetic showers in homogeneous ice, is described in Ref. [24]. The results of the simulation will be compared to those obtained using Eq. 4 with different curves for the excess charge development function  $Q(z)$  what will turn out to be quite illustrative.

Fig. 1 compares the angular distributions of the pulses for showers initiated by different energy electrons using the full simulation and using Eq. 4 with  $Q(z)$  directly from the excess charge depth distribution as obtained in the same simulations. Fig. 2 displays the frequency spectra at different observation angles for a 10 TeV shower again for both approaches. Several conclusions can be drawn from these graphs with respect to the validity of the 1-D approximation. Clearly the electric field amplitude around the Čerenkov cone is well reproduced in shape by the 1-D approximation except in the Čerenkov direction where the approximation overestimates the amplitude by a factor that increases with frequency. Below 100 MHz the effect is negligible becoming of order 20% (a factor of 2) for 300 MHz (1 GHz). The angular interval over which the approximation is valid slowly increases with shower energy and scales with the inverse of the frequency. Well outside the Čerenkov cone no agreement can be claimed but the order of magnitude of the approximation agrees with the simulation.

For completeness we give a new parameterization for the frequency spectrum in the Čerenkov direction using a finer subdivision of individual electron tracks (approximation *a* see appendix A), which represents slight increase at frequencies above 500 MHz from that given in Ref. [24]:

$$R|\vec{E}(\omega, R, \theta_C)| \simeq 2.53 \times 10^{-7} \left[ \frac{E_{\text{em}}}{1 \text{ TeV}} \right] \left[ \frac{\nu}{\nu_0} \right] \left[ \frac{1}{1 + (\nu/\nu_0)^{1.44}} \right] \text{ V MHz}^{-1} \quad (6)$$

where  $\nu_0 = 1.15$  GHz. This parameterization is valid to frequencies below  $\sim 5$  GHz.

It is worth discussing the interpretation of the behavior of this approximation before we attempt to understand its validity in more complicated showers such as those having strong LPM effects [27,28]. In the Čerenkov direction, corresponding to  $p = 0$ , the agreement between the approximation and the full simulation is excellent for frequencies below about 100 MHz. This corresponds to complete constructive interference characterized by a spectrum that increases linearly with frequency as shown in Fig. 2. Above 100 MHz the simulated frequency spectrum deviates from linear behavior because the wavelength becomes comparable to the transverse deviation of shower particles [24,29] and to a lesser extent because of time delays \*. Both these effects are ignored in the 1-D approximation that keeps on rising linearly. Away from the Čerenkov cone the approximation becomes valid even to higher frequencies. This is because destructive interference is in this case due to the longitudinal excess charge distribution which is correctly taken into account by the approximation.

In spite of the approximation overestimating the amplitude of the electric field in the Čerenkov direction for frequencies above  $\sim 100$  MHz, an ad-hoc correction can be implemented based on the shape of the frequency spectrum as obtained in the simulations. Since this effect is due to the lateral distribution of the electromagnetic component of the showers, it can be corrected with a unique function for each frequency. We have explicitly checked that the lateral distribution of electromagnetic showers is similar for showers with and without the LPM effect [22,30].

We have calculated the difference between the 1-D approximation and the full simulation in the Čerenkov direction as a function of frequency what is shown in Fig. 3 for two different shower energies. Note that the difference is (up to a factor that scales with shower energy)

---

\*It has been checked by direct simulation that the time delays only become important for frequencies in the 10 GHz range at the Čerenkov direction.

the same for showers of different energies. For this calculation we have actually improved the simulation by splitting the individual tracks in small subintervals (approximation *c*, see appendix A). Also shown is the calculation without track subdivisions (approximation *a*) for comparison. The angular behavior of the correction at a particular frequency can be also shown to be fairly independent of energy.

The needed correction basically consists of rescaling the pulse just in the region around the Čerenkov direction. It can be achieved for instance dividing the result of Eq. 4 by a gaussian correction factor:

$$1 + \left[ \frac{1D - FS}{FS} \right] e^{-\frac{1}{2} \left[ \frac{\theta - \theta_C}{\sigma_\theta} \right]^2} \quad (7)$$

The expression in brackets symbolically represents the relative difference between the frequency spectra as given by the 1-D approximation (*1D*) and the full simulation (*FS*) calculated in the Čerenkov direction. It simply sets the scale of the correction. The numerator is shown in Fig. 3 for two test cases, showing that it also scales with energy at least in the energy interval checked. The half width of the gaussian term is approximately given by:

$$\sigma_\theta = 2.2^\circ \left[ \frac{1 \text{ GHz}}{\nu} \right] \quad (8)$$

For frequencies above the 100 MHz scale and high energies when the full simulation is not viable, one would implement the correction taking Eq. 6 instead of the full simulated result.

The 1-D approximation also works for complicated showers such as those initiated by electrons and photons of EeV energies with strong LPM effects [22]. This has been explicitly checked by artificially lowering  $E_{\text{LPM}}$ , the onset energy for LPM effects, so that showers with energies that allow full three dimensional simulations display the characteristic LPM elongations [29]. The agreement between the full simulation and the 1-D approximations is illustrated in Fig. 4 and it is clear that it is not limited to the central peak but also applies to the secondary peaks that appear in the angular distribution of the radiated pulse. The above correction prescription also works for these fictitious elongated showers with a mild reduction in precision.



Lastly, the simulation of the excess charge in an EeV shower can also be extremely time consuming because particles have to be followed at least to MeV energies when the interactions responsible for the excess charge become dominant over pair production and bremsstrahlung [24]. According to simulations the pulse scales with the excess tracklength and this is practically only due to an excess of MeV electrons. The excess number of electrons can be approximately obtained by rescaling the total number of electrons and positrons in a shower by the fraction of excess and total tracklengths. This factor is very stable and has a value of 25% in ice [24]<sup>†</sup>. As convenient parameterizations of the number of electrons and photons in showers are readily available it is possible to calculate shower size distributions for very large showers using them [22,23]. In spite of the small gradual rise in the excess charge as the shower develops shown by simulations [24], the effects of this approximation are mild, a slight narrowing of the pulse which is negligible compared to the other approximations made (see Fig. 5).

Finally it is remarkably fortunate that neglecting lateral distributions and time delays is a very good way of approaching the problem if some considerations are cautiously taken into account, namely:

- Take the Fourier transform of the longitudinal distribution of the excess charge  $Q(z)$  (or one fourth of the total number of electrons and positrons if  $Q(z)$  is not available) as given by Eq. 4.
- For frequencies above 100 MHz divide the 1-D approximation by a correction factor as indicated by Eq. 7 taking Eq. 6 instead of the full simulation ( $FS$ ) value.

---

<sup>†</sup>This value corrects the previous conservative estimates used in [18] that quoted instead the ratio of excess projected tracklength to total tracklength as the relevant number (21%).

### A. Discussion: The relation between radio pulses and shower fluctuations

In the 1-D approximation the Fourier transform for  $p = 0$  becomes the integral of  $Q(z)$ , i.e. the excess tracklength. Simulations have shown that the excess tracklength scales extremely well with electromagnetic energy in the shower ( $E_{\text{em}}$ ) for both electromagnetic and hadronic showers up to energies exceeding 100 EeV with small fluctuations:

$$t = 6400 \left[ \frac{E_{\text{em}}}{1 \text{ TeV}} \right] \text{ m} \quad (9)$$

Incidentally this nice property of the excess charge together with the fact that the radioemission in the Čerenkov direction is proportional to the excess tracklength, make such measurements excellent candidates for electromagnetic energy estimators. The breaking of the approximation at high frequencies is telling us that the lateral distribution is playing a significant role.

A simple limit of the 1-D approximation is obtained by taking an analytical expression for  $Q(z)$  such as Greisen’s parameterization for the average development of an electromagnetic shower [31]. The result just gives the radiation in the Čerenkov cone but no radiation outside, just like the Fourier transform of a gaussian.

Invoking superposition we can subtract from a given shower development curve a smooth Greisen-like curve having the same tracklength. The result displays the “roughness” of the depth development curve and we shall refer to it as the *difference function*. The electromagnetic pulse is the sum of an isolated Čerenkov peak due to the Greisen-like curve and an extra contribution from the Fourier spectrum of the difference function which precisely vanishes at the Čerenkov direction because it does not contribute to the total tracklength. Moreover, for ordinary showers the amplitude of the difference function becomes smaller relative to shower size as the shower energy increases. This is just an statistical effect of having a larger number of particles and it indicates that the “spatial correlations”<sup>‡</sup> contained

---

<sup>‡</sup>The name stresses the fact that they are different from standard fluctuations in shower theory

in the difference function must be related to fluctuations in shower size.

The fact that the magnitude of the difference function becomes smaller relative to shower size as the shower energy  $E_0$  increases has the effect of "illuminating" the Čerenkov cone much more sharply with respect to directions well outside the Čerenkov direction. This effect can also be understood in terms of coherence. In the Čerenkov direction of greatest coherence the electric field amplitude scales with the shower energy  $E_0$ , but when the radiation is incoherent, i.e. well outside the Čerenkov direction, the electric field should add incoherently and hence scale with  $\sqrt{E_0}$ . This roughly agrees with simulations and nicely connects the properties of the radio emission to spatial correlations in shower development.

For LPM showers the structure of the pulse outside the central narrow peak is still dominated by the longitudinal development of these showers because the amplitude of the difference function is much larger than for a conventional shower. This is because LPM showers fluctuate a great deal. (One can picture a characteristic LPM shower as a superposition of smaller subshowers with typical smooth profiles with random starting points along the shower length.)

In other words, the Fourier modes of the excess charge distribution are probed by the electric field at a given value of  $p$  and hence at a given value of  $\theta$  for a fixed frequency. The scale of the correlations in the distribution (the "wavelength" of the corresponding mode) is inversely proportional to  $p$ . As long as the scale of these correlations is larger than the characteristic lateral structure of the shower, the 1-D approximation is expected to work. This is precisely what happens for the LPM fluctuations.

In summary there are two angular regions for the electromagnetic pulse with a not very well defined boundary. One angular region corresponds to the surroundings of the Čerenkov cone where the 1-D approximation has powerful predictive power when one accounts for the

---

because they refer to variations in shower size for the same shower at different positions rather than comparing shower size at the same spatial position for different showers.

correction described above. There is another region well outside the Čerenkov cone in which the calculated electric field amplitude drops considerably and behaves erratically, as some kind of “white noise” corresponding to the incoherent regime. In this region the short scale correlations of the excess track distribution are being probed and here the predictive power is lost with the approximations discussed. To calculate the radiopulse in such regions one needs three dimensional simulation programs which must sample tracks in small subintervals and which must follow all particles to the 100 keV region (approximation *c* described in appendix A). All these requirements make it impossible with current computing power to simulate beyond 100 TeV. However the region outside the Čerenkov cone, having much reduced radioemission, is not very relevant for shower detection.

#### IV. THE VALIDITY OF THE FRAUNHOFER APPROXIMATION

All the calculations made of radio pulses have been made in the Fraunhofer approximation which corresponds to the limit:

$$R > R_F = 3 \text{ m} \left[ \frac{L_s}{1 \text{ m}} \right]^2 \left[ \frac{\nu}{1 \text{ GHz}} \right] \quad (10)$$

Taking  $L_s \sim 3.8 \text{ m}$ , corresponding to the nominal ten radiation lengths in ice of a electromagnetic (hadronic) shower below about 10 PeV (10 EeV), a frequency of 1 GHz and  $\theta$  equal to the Čerenkov angle then  $R_F \sim 45 \text{ m}$ . This distance is to be compared with the km scale set by the small absorption coefficient of radio waves in cold ice which tells us that the Fraunhofer condition is clearly satisfied. For very long showers (such as those that display a very strong LPM effect) and high frequencies,  $R_F$  exceeds the typical attenuation scale. As the distance  $R$  is reduced to values below  $R_F$ , the diffraction pattern gradually turns into a Fresnel pattern in which the angular features become blurred.

It is possible to calculate diffraction patterns for such showers with the typical restrictions that apply to these simulations. A full calculation is again not viable for the shower energies at which this effect becomes important at km scale distances. We have calculated the radio

pulses as observed at distances in which the Fraunhofer approximation breaks down, using simulated electron showers of different energies. We apply Eq. 3 for calculating electric field amplitudes at distances of order the Fresnel distance  $R_F$ , (a one dimensional transform that does not take the Fraunhofer limit). We calculate the effects for a range of energies and observation distances to specify the conditions under which the properties of the emission in the Fraunhofer limit are still valid.

In Fig. 6 we display the Čerenkov peak structure at 100 MHz for a range of distances around the Fraunhofer limit for a 1 EeV electromagnetic shower spanning 135 radiation lengths. We define the distance in relation to the center of charge of the shower. The calculated pattern has a reduced amplitude at the peak and becomes broader as expected. The Fraunhofer approximation is good to better than 10% in absolute value for distances above  $\sim 400$  m. For a 100 EeV (10 PeV) shower the distance increases to 5 km (decreases to 20 m) for a roughly similar accuracy. The angular width of the pulse in the near field case increases with respect to the Fraunhofer case roughly by 20% when the amplitude reduces by 10%.

In Fig. 7 we plot the ratio of the calculated and Fraunhofer amplitudes at the Čerenkov peak as a function of distance to the shower for different frequencies and shower energies. Also indicated are the absorption lengths at three different temperatures for reference. This graph summarizes the results, for 1 km distance and energies above a few hundred PeV, Fresnel effects will become a serious concern for GHz frequencies. Provided that the distance to the shower and its direction can be determined, Fresnel effects could be corrected for, but this would clearly complicate and limit the analysis. This suggests that lower frequencies in the 100 MHz or even below may be appropriate for EeV showers. For hadronic type showers however no effects are foreseen for energies up to the 10 EeV range except for few abnormally long showers that are unlikely to happen [23].

## V. SUMMARY AND CONCLUSIONS

We have shown that the calculation of coherent Čerenkov radio pulses from high energy showers in ice in the Fraunhofer limit can be well approximated by neglecting the lateral distributions of the particles assuming that they travel at constant speed ( $c$ ). The electric field amplitude simply becomes the one dimensional Fourier transform of the excess charge depth distribution. For the most relevant region around the Čerenkov direction, the approximation is correct for frequencies below 100 MHz. At higher frequencies the approximation is still relatively good but systematically overestimates the pulse in the Čerenkov direction. We have shown that the model can be made to agree at least up to 1 GHz by subtracting a simple ad-hoc gaussian correction that is proportional to the shower energy and otherwise only dependent on frequency. We have reported the relevant parameters for the correction and have presented an improved parameterization for the electric field amplitude in the Čerenkov direction.

We have also shown that instead of the actual charge excess distribution one can use the shower size longitudinal development curve which is more conventional than the excess charge, scaling the amplitude of the central peak by the excess tracklength fraction 0.25.

We have developed a similar approximation for the region in which the Fraunhofer limit ceases to be valid. We have finally studied the behavior of the radiopulses of long electromagnetic showers in this region. Our results are again suggesting to use low frequencies for EeV showers as concluded in Ref [18]. These frequencies have a number of advantages because they are less attenuated, they allow observation of the angular structure with less detectors, and they have milder Fresnel effects at a given distance. Because of Fresnel corrections, the possibility of extracting the mixed character of electron neutrino interactions suggested in [18] requires frequencies below 100 MHz if the electron initiated subshower exceeds about 10 EeV.

Lowering the frequency implies a higher threshold for detection because the Čerenkov spectrum increases with frequency but for EeV showers this should not be a problem. It

has been estimated that the threshold for detecting showers at 1 km distance with 1 GHz broadband antennas is in the 10 PeV range [24]. Since the signal to noise roughly scales with the square root of the bandwidth which directly relates to the central frequency, a factor of 100 reduction in frequency will only call for about a factor of 10 enhancement of the threshold still giving a very large signal to noise ratio for EeV showers.

Although our tests of the 1-D approximation rely heavily on a specific simulation program [24], our claim on the validity of the 1-D approximation is model independent. For testing purposes we used the charge excess distribution and the emitted radiopulses as obtained by the same routine. Numerically our results only apply for ice but it is only natural to expect that the same procedures can be applied to calculate the radiation in other materials.

**Acknowledgements:** We thank P. Gorham for many early discussions about Fresnel corrections and D. Besson, D.W. McKay, J.P. Ralston, S. Razzaque, D. Seckel and S. Seunarine for constructive criticism of the Montecarlo and many discussions. This work was supported in part by CICYT (AEN99-0589-C02-02) and by Xunta de Galicia (XUGA-20602B98). J. A. thanks the Department of Physics, University of Wisconsin, Madison and the Fundación Caixa Galicia for financial support. E. Z. thanks the Department of Physics, University of Wisconsin, Madison, where this work was finished for its hospitality, and the Xunta de Galicia for partially supporting this trip.

## APPENDIX A: The ZHS Montecarlo

The simulation program used described in [24] is a specifically devised program for calculating radio-pulses from electromagnetic showers that follows particles to  $\sim 100$  keV, taking into account low energy processes and timing. The depth development results have been compared to analytical parameterizations given in the Particle Data Book [32], with which they agree to a few percent.

The calculation of the radio emission uses Eq. 5 for electron and positron tracks. Several approximations can be made according to different choices in the subdivision of the individ-

ual charged particle tracks. In Ref. [33] three different choices, named approximations  $a$ ,  $b$ , and  $c$  have been compared, testing for convergence as the subtracks become smaller.

Approximation  $a$  is the standard that has been used in Refs. [24,34]. It corresponds to taking the end points of all the tracks, and it just uses the average velocity for the corresponding effective track in Eq. 5. This is the standard reference calculation used throughout in this article except for Fig. 3. Note that this approximation gives the correct result provided the particle velocity is constant along the track.

Approximation  $b$  subdivides the electron tracks according the different interaction points found along the track, (multiscattering is not considered as an interaction here). This approximation subdivides the track in finer subintervals as the energy becomes smaller, because the low energy electron scattering cross sections exceed bremsstrahlung and pair production. For each subtrack the average velocity is calculated between the corresponding end points of the track. Finally approximation  $c$  subdivides each interaction according to a convenient algorithm for splitting the propagation of particles designed to better calculate the multiple scattering at low energies.

The three approximations are compared in Fig. 8 illustrating the convergence of the method and how the approximation  $a$  is valid in the Čerenkov cone to a precision better than about 10% for frequencies below 1 GHz. Full simulations in approximation  $c$  are much more time consuming and have to be done for shower energies below  $\sim 100$  TeV. At low energies fluctuations from shower to shower are more important so that these tests are inevitably subject to larger uncertainties because of such fluctuations.

## APPENDIX B: The gaussian approximation

For electromagnetic (hadronic) showers below 10 PeV (10 EeV), that is having no important deviations from Greisen behavior, the electric field around the Čerenkov cone can be accurately determined with a gaussian approximation. The precise width of the cone inversely relates to the width (in  $z$ ) of the excess charge depth distribution,  $Q(z)$ . As  $p$  is directly related to the observation angle  $\theta$  with an expression that involves the frequency



as an overall factor, the width of the angular distribution of the "central peak" becomes inversely proportional to  $\omega$ .

For small deviations from the Čerenkov angle ( $\Delta\theta$ ) the expression for  $p$  to first order is [18]:

$$p = \frac{\omega}{c} \sqrt{n^2 - 1} \Delta\theta + O(\Delta\theta^2) \simeq 30.8 \left[ \frac{\nu}{1 \text{ GHz}} \right] \Delta\theta \text{ (m}^{-1}\text{)} \quad (11)$$

The numerical value given in this expression corresponds to showers in ice with  $n = 1.78$ . Defining the gaussian width by the points in which the amplitude drops by a factor  $\sqrt{e}$  a gaussian of half-width  $\sigma_z$  transforms to another gaussian of half-width  $\sigma_p = (\sigma_z)^{-1}$ . We can fit a gaussian to the excess charge depth development curve identifying the *shower length* by the width  $l = 2\sigma_z$  and the angular full width of the radiopulse is then:

$$\sigma_\theta \simeq 3.72^\circ \left[ \frac{1 \text{ GHz}}{\nu} \right] \left[ \frac{1 \text{ m}}{l} \right] \quad (12)$$

using approximation given by Eq. 11. For a typical shower length of 8 radiation lengths ( $\sim 3.1 \text{ m}$  in ice) the angular width of the pulse is about  $1^\circ$  at 1 GHz, in agreement with Ref. [24].

## REFERENCES

- [1] T.K. Gaisser, F. Halzen, and T. Stanev, Phys. Rep. **258**, 173 (1995).
- [2] K. Mannheim, Astropart. Phys. **3**, 295 (1995).
- [3] E. Waxman and J. N. Bahcall, Phys. Rev. Lett. **78**, 2292 (1997).
- [4] V.S. Berezinsky, M. Kachelriess and A. Vilenkin, Phys. Rev. Lett. **79**, 4302 (1997).
- [5] P. Bhattacharjee and G. Sigl Phys. Rep. **327** (3-4), 109 (2000).
- [6] M. Birkel and S. Sarkar, Astropart. Phys. **9**, 297 (1998).
- [7] P. Bhattacharjee, C.T. Hill and D.N. Schramm, Phys. Rev. Lett. **69**, 567 (1992); R.J. Protheroe and T. Stanev, Phys. Rev. Lett. **77**, 3708 (1996).
- [8] M. Ave, J.A. Hinton, R.A. Vazquez, A.A. Watson and E. Zas, submitted to Phys. Rev. Lett.
- [9] F. Halzen, R.A. Vazquez, T. Stanev and H.P. Vankov, Astrop. Phys. **3**, 151 (1995).
- [10] D.J. Bird *et al.*, Phys. Rev. Lett. **71**, 3401 (1993).
- [11] F.W. Stecker, C. Done, M.H. Salamon and P. Sommers, Phys. Rev. Lett. **66**, 2697 (1991); Errata, Phys. Rev. Lett. **69**, 2738 (1992).
- [12] F. Halzen *et al.* (AMANDA collaboration), Nucl. Phys. Proc. Suppl. **77**, 474 (1999); C. Arpesella (ANTARES collaboration), Nucl. Instrum. Meth. A **409**, 454 (1998); BAIKAL Collaboration, talk presented at the 18th International Conference on Neutrino Physics and Astrophysics (Neutrino 98), Takayama, Japan, June 1998; NESTOR collaboration, *Proc. XXVI Int. Cosmic Ray Conference*, Salt Lake City, Utah, U.S., Vol. 2, p. 456.
- [13] G.A. Askar'yan, Zh. Eksp. Teor. Fiz **41**, 616 (1961) [Soviet Physics JETP **14** 441, (1962)]; **48**, 988 (1965) [**21**, 658 (1965)].
- [14] G.M. Frichter, J.P. Ralston, D.W. McKay, Phys. Rev. D **53** 3, 1684 (1996).

- [15] A.L. Provorov, I.M. Zheleznykh, *Astrop. Phys.* **4**, 55 (1995).
- [16] P.B. Price, *Astrop. Phys.* **5**, 43 (1996).
- [17] M.A. Markov and I.M. Zheleznykh, *Nucl. Instr. and Methods in Phys. Research* **A248** 242, (1986).
- [18] J. Alvarez-Muñiz, R.A. Vázquez and E. Zas, *Phys. Rev. D* **61**, 023001 (1999).
- [19] J.V. Jelley, *Astroparticle Physics* **5**, 255 (1996).
- [20] P. Gorham, D. Saltzberg, P. Schoessow, M. Conde, W. Gai, J. Power and R. Konecny, (in preparation).
- [21] G.M. Frichter *Proc. XXVI Int. Cosmic Ray Conference*, Salt Lake City, Utah, U.S., Vol. 2, p. 467; see also <http://rice.bartol.udel.edu>.
- [22] J. Alvarez-Muñiz, E. Zas, *Phys. Lett.* **B411**, 218 (1997).
- [23] J. Alvarez-Muñiz, E. Zas, *Phys. Lett.* **B434**, 396 (1998).
- [24] E. Zas, F. Halzen, T. Stanev, *Phys. Rev. D* **45**, 362 (1992).
- [25] H.R. Allan, *Progress in Elementary Particles and Cosmic Ray Physics* (North Holland, 1971), Vol. 10, p. 171.
- [26] J.D. Jackson, *Classical Electrodynamics*. 2<sup>nd</sup> edition, John Wiley and Sons, Inc, 1975.
- [27] T. Stanev et al. *Phys. Rev. D* **25**, 1291 (1982).
- [28] S.R. Klein, *Rev. Mod. Phys.* **71**, 1501 (1999).
- [29] J. Alvarez-Muñiz, PhD. thesis, University of Santiago de Compostela, Spain, (July 1999).
- [30] J. Alvarez-Muñiz and E. Zas (in preparation).
- [31] K. Greisen, in: *Prog. of Cosmic Ray Phys.*, ed. J.G. Wilson, Vol. III, (North Holland

Publ. Co., Amsterdam, 1956) p.1.

[32] C. Caso et al, Eur. Phys. J. **C3**, 1 (1998).

[33] J. Alvarez-Muñiz, G. Parente, and E. Zas, *Proc. XXIV Int. Cosmic Ray Conference*, Rome (Italy) July 1995, Vol. 1 p. 1023.

[34] F. Halzen, E. Zas, T. Stanev, Phys. Lett. B **257**, 432 (1991).

# FIGURES

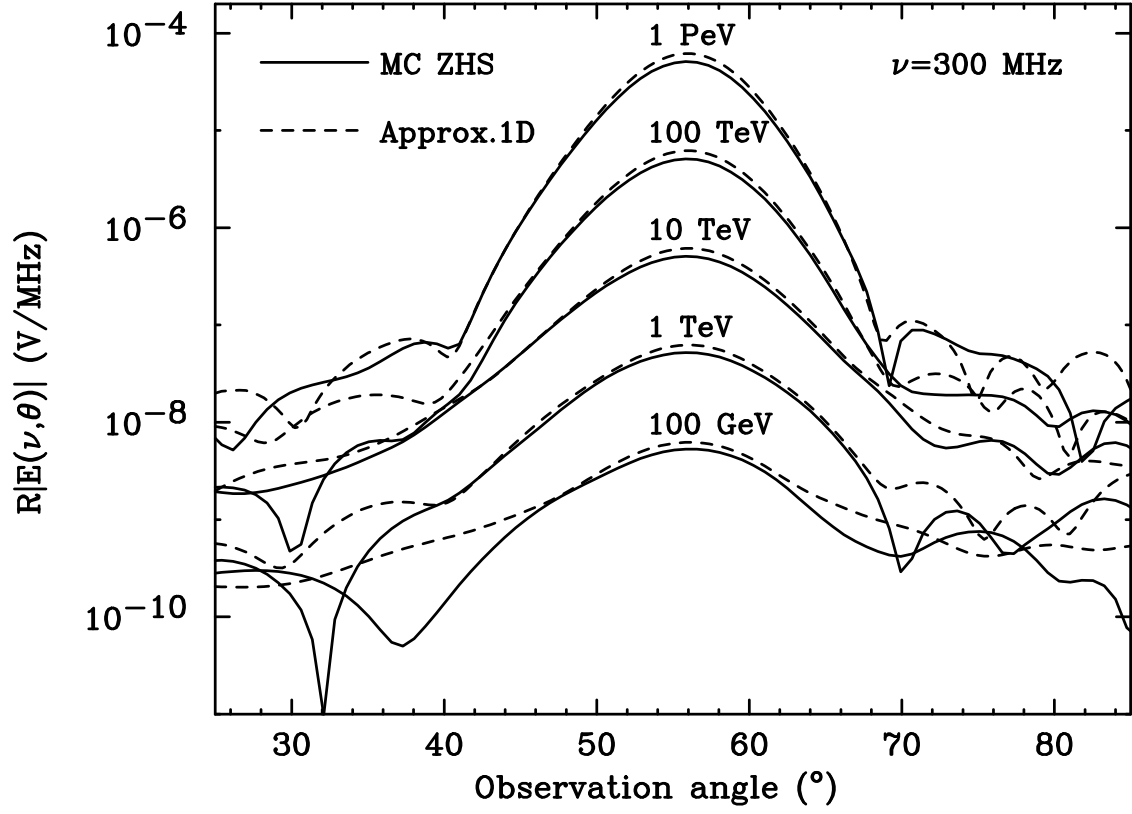


FIG. 1. Comparison of results of the 1-D approximation to fully simulated pulses for electromagnetic showers of 100 GeV, 1 TeV, 10 TeV, 100 TeV and 1 PeV. Simulations have been followed to threshold energy  $E_{th} = 1$  MeV. Shown is the angular distribution of the electric field amplitude for 300 MHz in the Fraunhofer limit multiplied by observation distance.

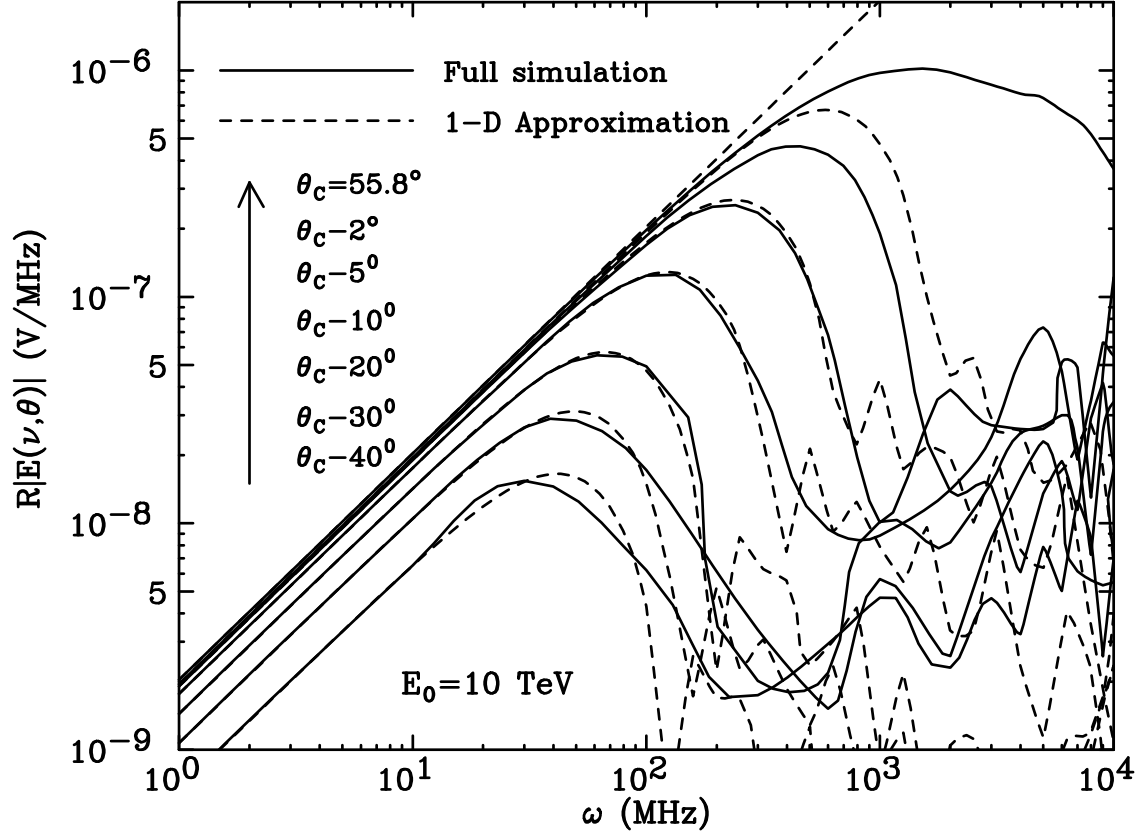


FIG. 2. Comparison of results of the 1-D approximation to fully simulated pulses for a 10 TeV shower with  $E_{th} = 611$  keV. Shown is the frequency spectrum of the electric field amplitude for different observation angles.

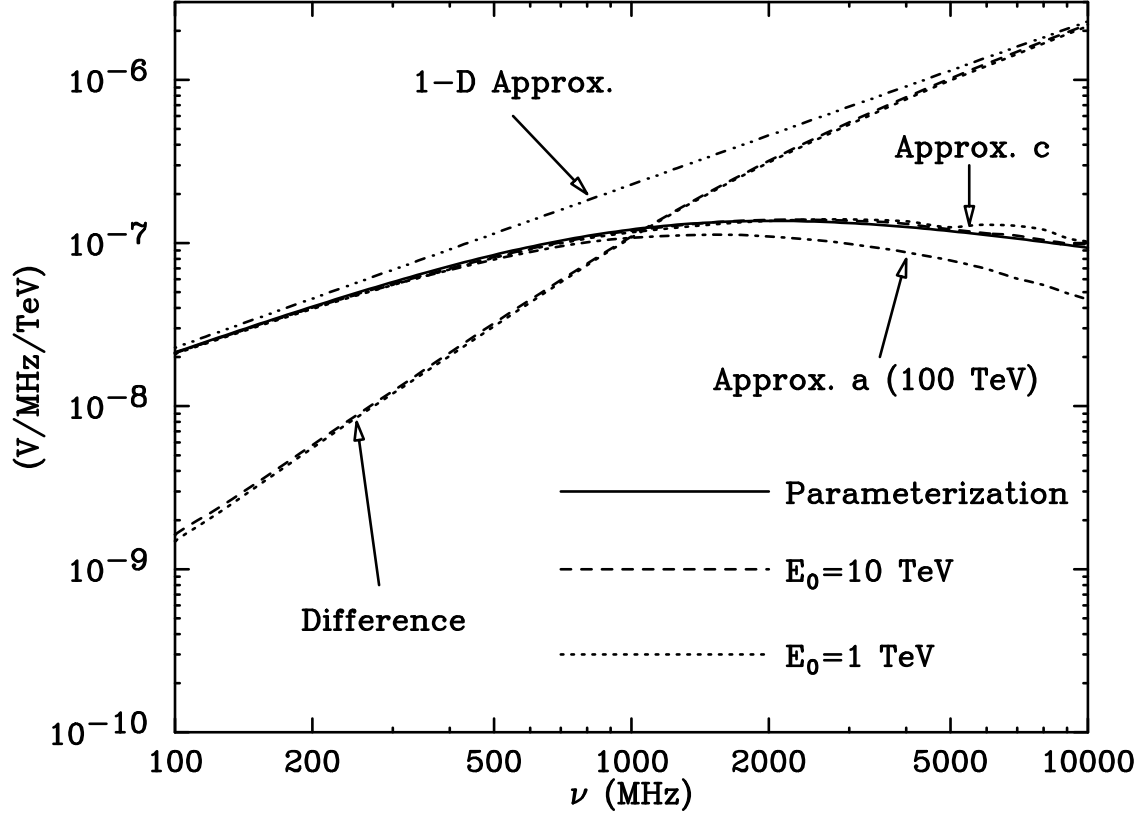


FIG. 3. Full simulation results for the frequency spectrum in the Čerenkov direction for 1 and 10 TeV electromagnetic showers in approximation  $c$  and for a 100 TeV in the standard approximation ( $a$ ) used throughout for comparisons (see appendix A). They are compared to the results using the 1-D approximation (top curve). The improved parameterization for the  $c$  approximation given by Eq. (6) is also shown. The lower curves represent the difference between the 1-D approximation and the full simulation results (using approximation  $c$ ). Note that both the spectrum and the difference have the same behavior for all shower energies. All radiopulses scale with shower energy and are normalized to 1 TeV.

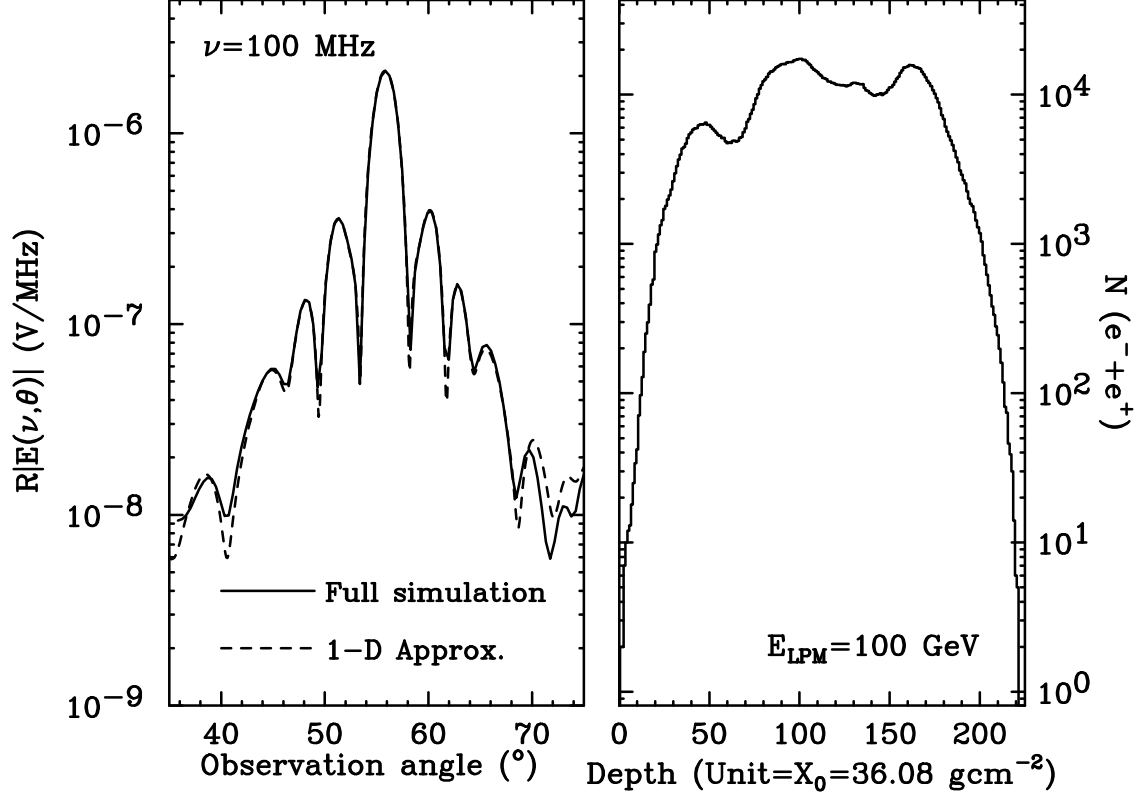


FIG. 4. Comparison of results of the 1-D approximation to fully simulated pulses for a fictitious composite shower that combines two 10 TeV subshowers initiated at the origin and one 100 TeV subshower starting at a depth of 25 radiation lengths. Furthermore these subshowers are artificially elongated by reducing the onset of the LPM effect ( $E_{\text{LPM}}=100 \text{ GeV}$  instead of the actual value for ice which is 2 PeV). The longitudinal shower profile is also shown.



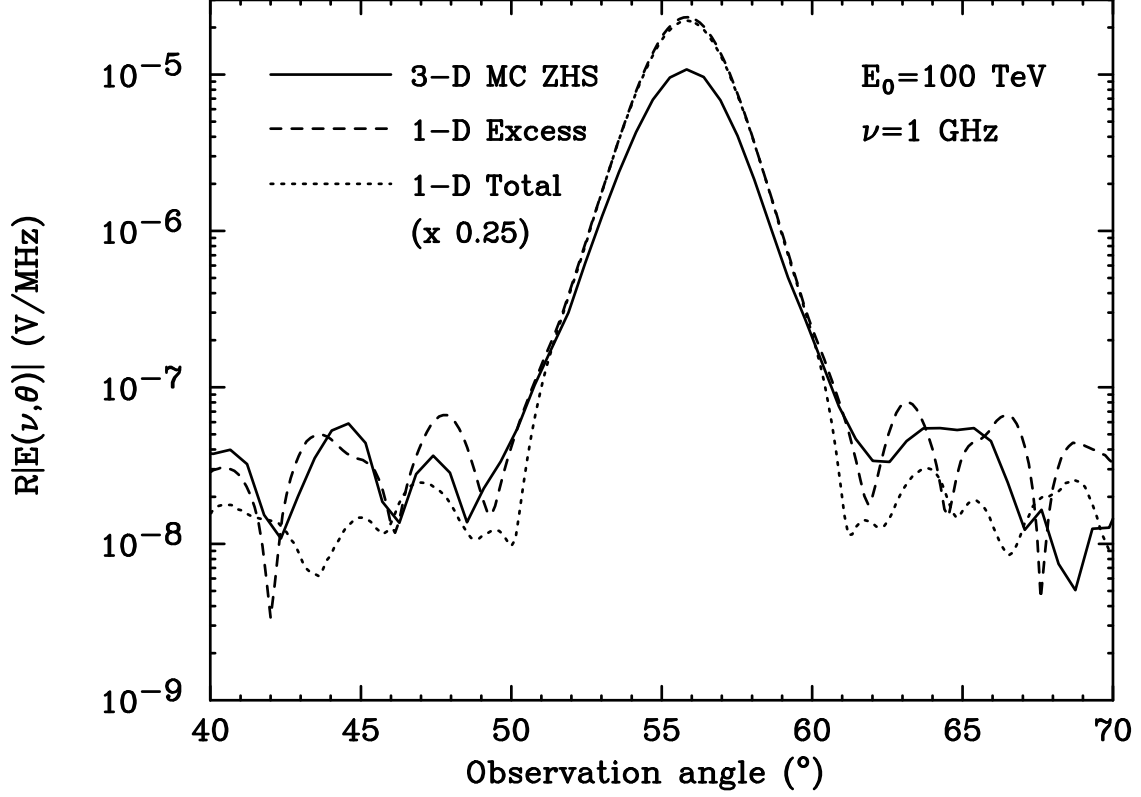


FIG. 5. Comparison of results of the 1-D approximation to a fully simulated pulse for an electron shower of 100 TeV. Simulations have been followed to threshold energy  $E_{th} = 611$  keV. Shown is the angular distribution of the electric field amplitude for 1 GHz in the Fraunhofer limit multiplied by observation distance. Two curves are shown for the 1-D approximation using the excess charge  $Q(z)$  and the shower size  $N(z)$  as obtained in the same simulation. The value obtained with shower size has been multiplied by 0.25 as explained in the text.

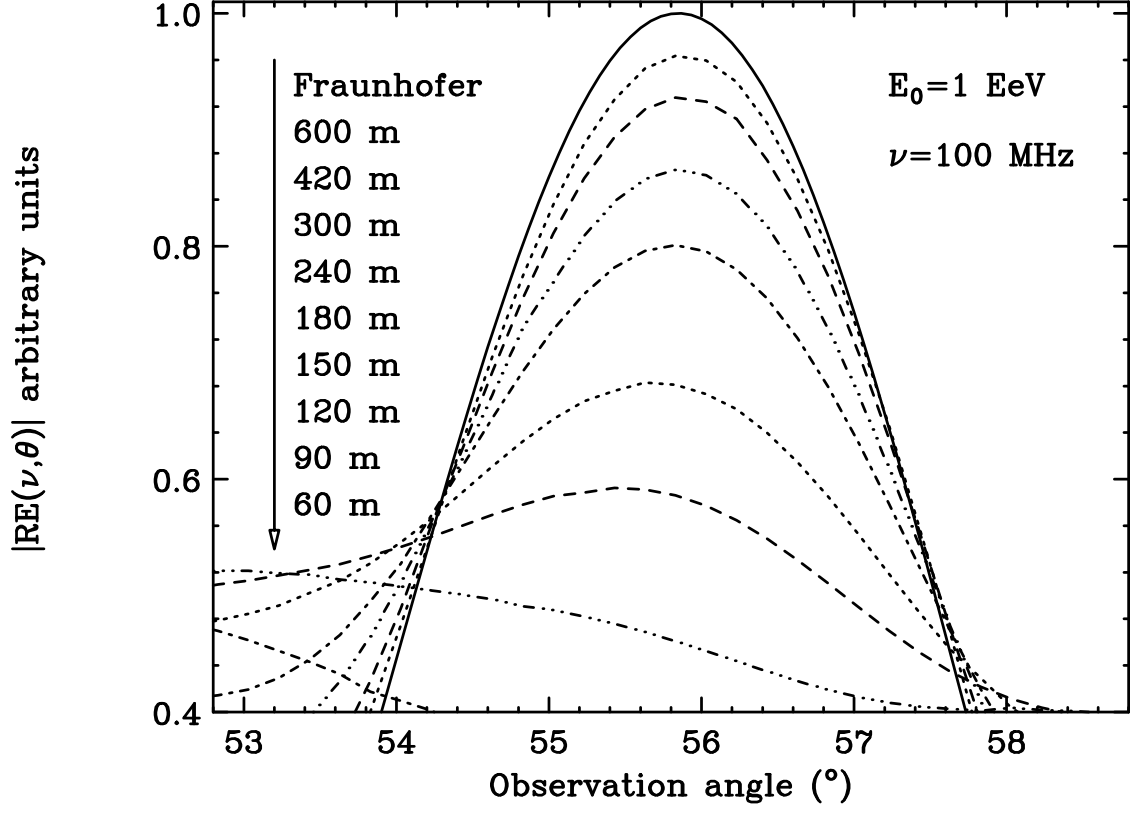


FIG. 6. Results of the 1-D approximation as the observation distance approaches the Fresnel distance  $R_F$  for a 1 EeV electromagnetic spanning 135 radiation lengths.

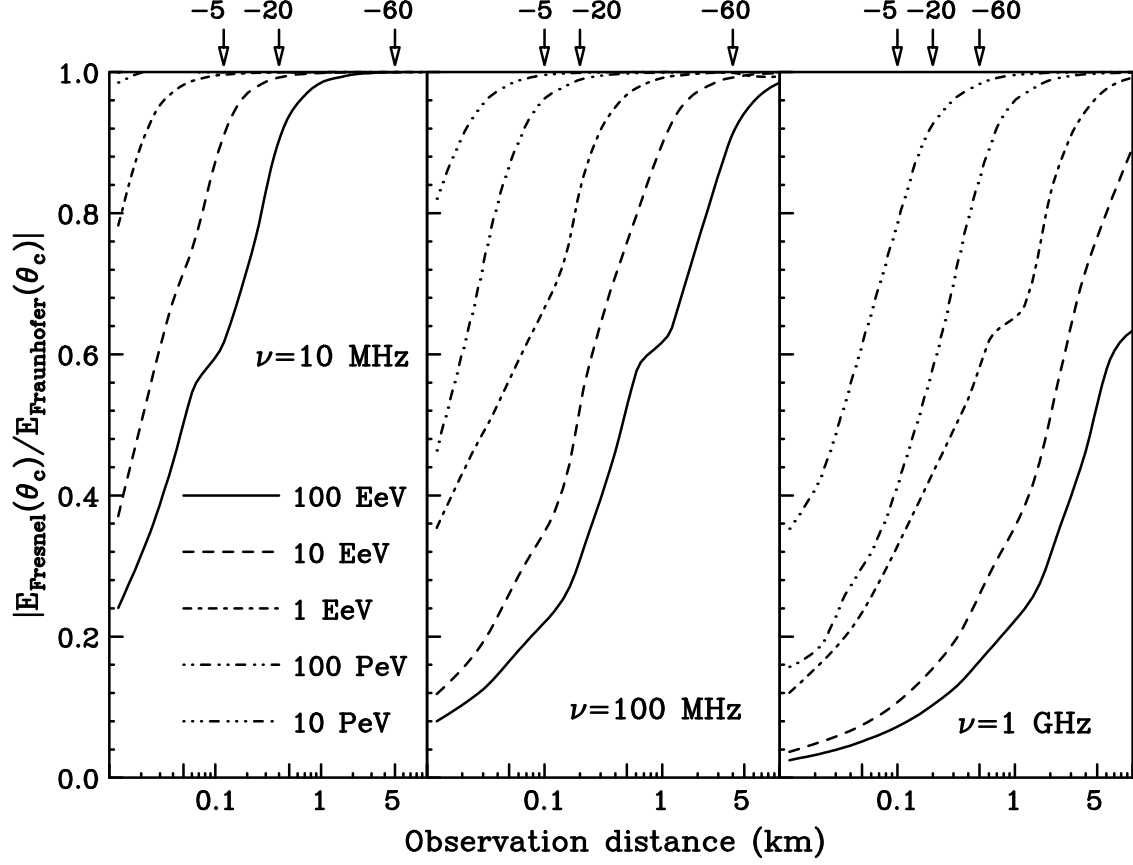


FIG. 7. Electric field amplitudes in the Čerenkov direction as a function of observation distance as obtained using the 1-D approach for different frequencies. The amplitudes are normalized to the amplitude in the Fraunhofer limit. The arrows indicate the attenuation lengths for the corresponding frequencies at three different reference temperatures (in  $^\circ\text{C}$ ).

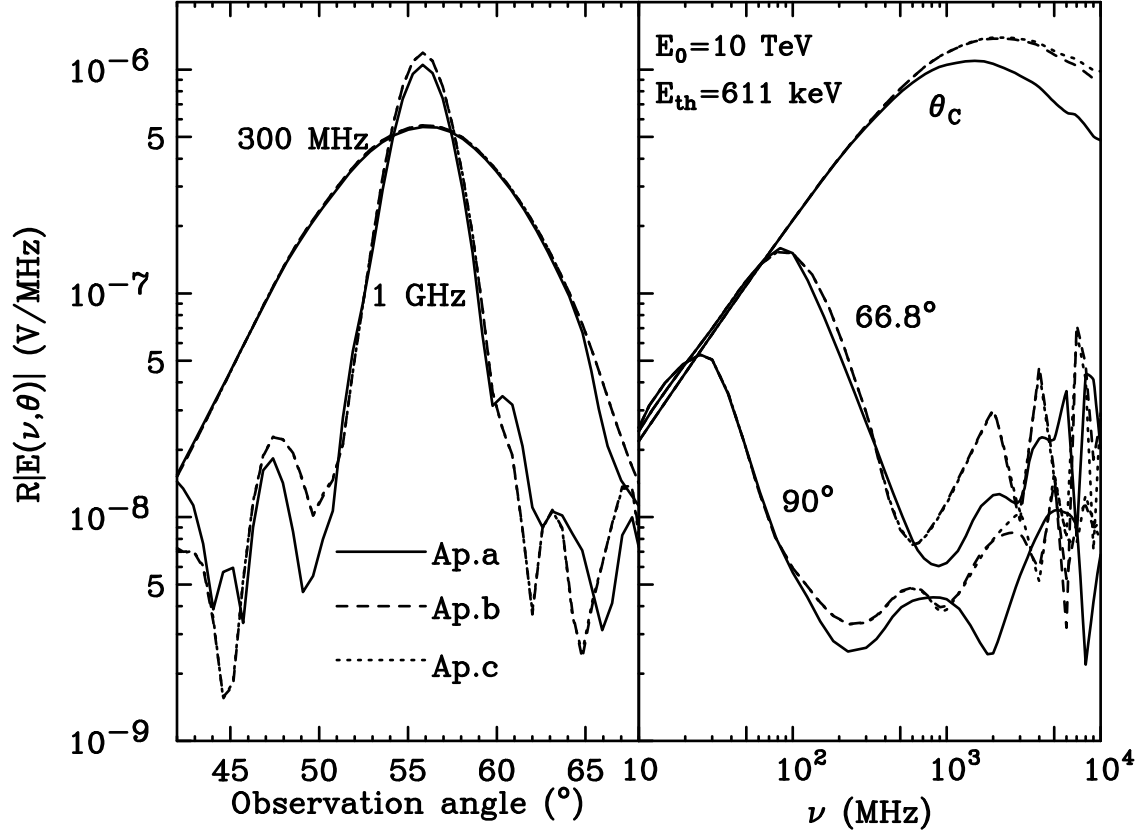


FIG. 8. Results of the full simulations with different algorithms for track subdivisions in the calculation of the electric field amplitudes as discussed in the text (appendix A). Shown are both the angular distributions for 300 MHz and 1 GHz and the frequency spectrum at three different observation angles for a 10 TeV electron shower with a threshold of 611 keV.